This article has been accepted for publication in a future issue of this journal, but has not been fully edited. Content may change prior to final publication. Citation information: DOI 10.1109/TII.2017.2773507, IEEE Transactions on Industrial Informatics

Autonomous Power Control and Management Between Standalone DC Microgrids

P Sanjeev, *SIEEE*, Narayana Prasad Padhy, *SMIEEE* and Pramod Agarwal, *MIEEE*

***Abstract*-- Renewable integrated DC Microgrids (DCMGs) are gaining popularity by feeding remote locations in qualitative and quantitative manner. Reliability of autonomous DC microgrids (ADCMG) depend on battery capacity and size due to stochastic behavior of renewables. Over charging and discharging scenarios compel the microgrid into insecure zone. Increasing the storage capacity is not an economical solution because of additional maintenance and capital cost. Thus interconnecting neighbor microgrids increases virtual storing and discharging capacity when excess power and deficit scenario arises respectively in any of the DCMG. Control strategy plays vital role in regulating the power within and between microgrids. Power control and management technique is developed based on bus signaling method to govern sources, storages and loads to achieve effective coordination and energy management between microgrids. Proposed scheme is simple and reliable since bus voltages are utilized in shifting the modes without having dedicated communication lines. Proposed scheme is validated through real time simulation of two autonomous DC grids in real time digital simulator (RTDS) and its results are validated by hardware experimentation.**

***Index Terms*-- Autonomous DC Microgrid, Bus signaling method, Power control and management scheme, Renewable sources, Real time simulation.**

I. Introduction

Isolated DC microgrids are gaining lot of interest from researchers in recent past[1]–[4] over counter parts available due to their merits in relieving from complexity control, synchronization issues, harmonics and reactive power[5]. In developing/undeveloped countries, domestic consumers, data center and telecommunication systems in remote locations are served by local DC grids instead of conventional grid since utility connection is not feasible or uneconomical[6]–[8]. Unlike to grid connected DC microgrid[9], there is no utility available in autonomous DC microgrids (ADCMGs) to balance power between generation and consumption. Thus effective coordination and control plays key role in ADCMGs to meet optimal energy management and efficient utilization of resources and storage units [10].

Control schemes based on centralized controller provide the optimal operation among various units by acquiring the information from them and manage the data centrally [11]. But system reliability is degraded due to high dependence on central controller and communication link. Droop control [12] is a basic decentralized control method which works based on local information but lacks with optimum utilization of resources of microgrid. To overcome above drawbacks, a distributed control strategy based on DC bus signaling method (DCBSM) was introduced in [13]. But it fails to consider the over charging and discharging of battery. In [14], state of charge (SoC) of battery is included in primary level control based on DCBSM. Secondary level control is designed for adjusting bus voltage as per the reference voltage. As the battery alone regulates the bus voltage, reliability of system degrades. In [15], decoupling the operating regions in primary level control is proposed using DC bus voltage levels. And, coordination among various storage devices is achieved in secondary level through communication. However, excess generation is inefficiently managed by using dump loads. Multilevel energy management strategy is proposed in [16], where hybrid storage devices are utilized to suppress both low and high frequency components during power variations. During over charging or discharging conditions, the hybrid storage devices are poorly managed if the communication fails among control levels.

Papers [17], [18]proposes the different control modes based on bus voltage deviation for regulating the DC microgrid under variable generation and storage. These papers utilize bus voltage for indicating status of DC microgrids. Both the papers consider the utility grid and assigns slack role to different sources (i.e. utility grid side converter or storage converter) in each mode based on conditions of DC microgrid and utility grid. Distinct control loops are employed under each mode for optimizing the system performance which requires frequent switching between control loops that causes switching transients and also increases burden on control processor. Besides this, excess power beyond the battery charging rate and grid side converter rating is not explored in [17]. Although it is considered by [18], but the deviation of bus voltage is more than 10% of nominal value in islanded mode which affects the sensitive loads connected. Power line signaling method is proposed in [19] to overcome problem of limited number of operating modes based on fixed voltage deviation in DCBSM. It dispatches the status of batteries and other sources in terms of distinct frequency signals superimposed on bus voltage. Various sources can shift their operating modes by extracting the information from different frequency signals. However this method is not suitable for increased number of storage systems (SS) and distributed energy resources (DER) since available carrier signal frequencies are limited and also varies based on different converter parameters, which makes proposed scheme cumbersome to implement for more number of DERs and SSs. Besides, it consumes additional current from battery for dispatching the various signals.

This work is supported by Department of Science and Technology (DST), India under the India-UK "Smart Energy Grid and Energy Storage (SEGES)" research initiatives.

Authors are with the Department of Electrical Engineering, Indian Institute of Technology, Roorkee, Uttarakhand, 247667, India, (e-mail: sanjeev.pannala@gmail.com; nppeefee@iitr.ac.in; pramgfee@ iitr.ac.in).

This article has been accepted for publication in a future issue of this journal, but has not been fully edited. Content may change prior to final publication. Citation information: DOI 10.1109/TII.2017.2773507, IEEE Transactions on Industrial Informatics

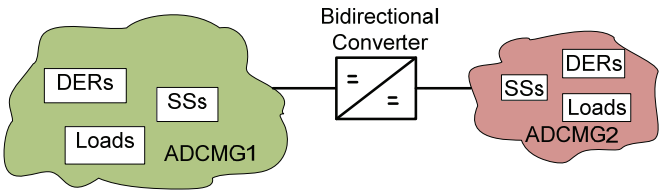

Fig. 1. Typical interconnection of two ADCMGs.

Above all, beyond the charging and discharging capacity of the storage devices in ADCMGs, when power surplus or deficit arises in the ADCMG, an additional storage system is required [20]. Increasing the SS will elevate system cost due to extra maintenance and initial setup cost. Besides, it introduces complexity in control which indirectly reduces reliability due to dependency on fast processing and communication technology between different storage units. In order to avoid the additional storage requirement, interconnection of DC grids is developed [21] similar to conventional AC systems (one area to other area) which enhances system reliability and make the efficient usage of resources. Typical structure for interconnecting ADCMGs is shown in Fig. 1. Each microgrid encloses distributed energy resources, storage systems and various loads.

Papers[21]–[30] describes about interconnection of DC microgrids. Paper[21] proposes decentralized power flow control between DC microgrid clusters using tie line connection based on bus voltage adjustment/ regulation without incorporating extra bidirectional DC-DC converter. Small deviation in bus voltages may yield unwanted power flow between the DC microgrids and also increases transmission losses. Various configurations for interconnecting the DC microgrid clusters are studied in [22] and a control strategy is proposed based on hierarchical control for regulating the power through interlinking bidirectional DC-DC converter between DC microgrids. As it embraces three control layers (i.e. primary, secondary and tertiary) which demands dedicated and fast communication channels between them for optimal power sharing among DC microgrids that makes system more costly and also increases burden on control processor. Three approaches(circuit switching, packet switching and virtual packet switching) are proposed in [23] for power sharing between DC microgrid clusters by taking analogy from internet architecture. They are analyzed in terms of their abilities and merits over other with four fundamental rules of internet. But it increases number of interlinking DC-DC converters and buffer storages which is not cost effective. In [24], interconnection of ADCMGs is explored by proposing centralized control strategy to ensure optimal operation of each grid using conventional non-isolated bidirectional DC-DC converter. System reliability heavily depends on centralized controller and communication link. This yields to single point of failure. Moreover, isolation between ADCMGs is not provided. Even though isolation inherently present in [25] due to flyback converter, but power sharing heavily depends on the gap between generation and demand that is similar to previous case which entails the communication from various units. In [26], a new DC-DC converter based on LCL filter is proposed by eliminating transformers in dual active bridge converter (DABC) for high power and high voltage transmission systems. Though it shows significant improvements in reducing the weight, losses and reactive power, but suits for high power and high DC voltage applications where the operating frequency is limited. Besides, it also lacks with galvanic isolation. Extended phase shift control is proposed for DABC in [27] to interface the low and medium voltage DC grids. Main focus lies on bidirectional power control and fails to consider the conditions of the individual DC grids. Design and operation of new bidirectional DC-DC converter enclosing CLLC resonant tank for zero voltage and zero current switching is explored in [28] for dissimilar voltage based DC buses but does not comment on the status of sources connected to individual DC buses which influences the power flow between the DC grids. Paper [29] proposed a strategy based on bus states for transferring the power between DC microgrids. As the droop control is employed for governing the distributed generation in single microgrid, scheme fails to extract the maximum power from renewable sources and demands central communication for optimal operation. Two-level tertiary control scheme is proposed in [30] for optimal power sharing among DC microgrids within the cluster by regulating reference voltages in DC microgrids. However, this scheme entails sparse communication and may yield to non-optimal power sharing between the DC microgrids either due to upper level communication failure or due to tracking errors during dynamic power variation of sources/loads within microgrids[31].

In this paper, a power control and management strategy (PCMS) is developed based on DCBSM for individual ADCMGs and as well as between ADCMGs without any dedicated communication infrastructure. Control and management of sources, storages and loads in PCMS are executed by using bus voltage information. Similarly both the bus voltages are used to trigger the DABC between the ADCMGs for power exchange. In addition, PCMS embraces extreme situations like over and under loading conditions of individual ADCMGs which are handled efficiently by running load shedding and PV derating algorithms respectively. PCMS is simple and communication free power control strategy within and between microgrids so that effective utilization and management of resources is achieved along with enhanced reliability of ADCMGs.

Paper is organized as follows: architecture of system is explained in section II. Proposed PCMS for ADCMGs is discussed in section III. Control loops for various converters and IBDC are elaborated in section IV. Simulation results are discussed in section V and are validated by experimental results in section VI. Section VII concludes the paper.

II. SYSTEM STRUCTURE

System contemplated in this paper is as shown in Fig. 2 which consists of two ADCMGs spatially apart from each other with considerable line resistance between them. Each ADCMG consists of one photovoltaic (PV) source and battery as equivalent to group of sources from renewable sources and storage devices family respectively in order to simplify the analysis for the proposed PCMS between the ADCMGs. As most of DC loads are of constant power loads (CPL) which are

This article has been accepted for publication in a future issue of this journal, but has not been fully edited. Content may change prior to final publication. Citation information: DOI 10.1109/TII.2017.2773507, IEEE Transactions on Industrial Informatics

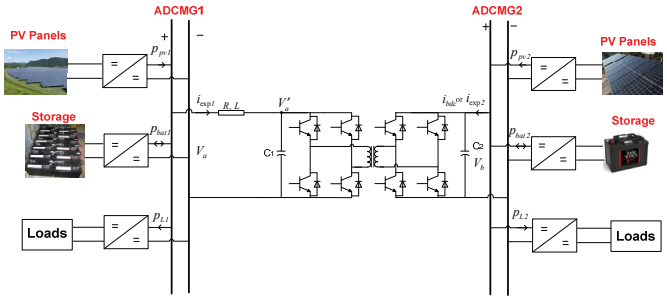

Fig. 2. System architecture for interconnection of two ADCMGs.

integrated through DC-DC converter. Hence, CPLs can able to maintain fixed power irrespective of variations in DC bus when its voltage oscillations lie within the sustainable range [15]. PV source is interfaced to DC bus through boost converter and bidirectional buck-boost DC-DC converter is utilized for connecting the battery storage. Interconnection of two ADCMGs is realized by considering DABC as interfacing unit which provides galvanic isolation and high power feeding capability in both directions along with large conversion ratios through high frequency transformer[27]. Two full H-bridge converters are connected to either side of the transformer to produce the high frequency AC from DC. Besides, this topology recognized as DABC and widely employed in transferring the power from low to high voltage DC [27].

As DABC is placed nearby low voltage DC grid (i.e. ADCMG2) to avoid losses, its bus voltage is directly available to DABC. Bus voltage information of other ADCMG (i.e. ADCMG1) is taken from the line connecting the two ADCMGs. Suppose the line is open, then voltage measured at capacitor C_1 (i. e. V_a') is considered as bus voltage of ADCMG1 for BDC triggering as there is no line drop. If the line is closed between two ADCMGs then the current measured in the line can be used to find out the voltage drop ($i_{exp1} \times R$) in the line. This voltage drop of the line can be further added to the voltage measured at high voltage side of the DABC (i.e. V_a') to estimate the exact voltage of ADCMG1. Hence, the voltage of ADCMG1 can be easily obtained without any communication link. Therefore ADCMGs can exchange the power among them based on bus voltages information available at DABC without dedicated communication systems. The following assumptions are made in the system.

1) Maximum capacity of PV source is higher than the rated battery charging power and load power to serve the loads most of the time through PV power.
2) Nominal bus voltage deviations are within the tolerance band of loads.

III. Power Control and Management Strategy (PCMS)

Source and storage units of ADCMGs are operated based on bus voltage levels in the grid by making bus voltage as information carrier between the units for proper coordination and management. Loads are managed depending on the state of charge (*SoC*) of battery and power condition of ADCMG which is expressed in terms of bus voltage deviation. Instantaneous *SoC* can be estimated by using coulomb counting method[32]:

$$SoC_i = SoC_0 - \frac{1}{C_N}\int \delta i_{bat}\, dt \qquad (1)$$

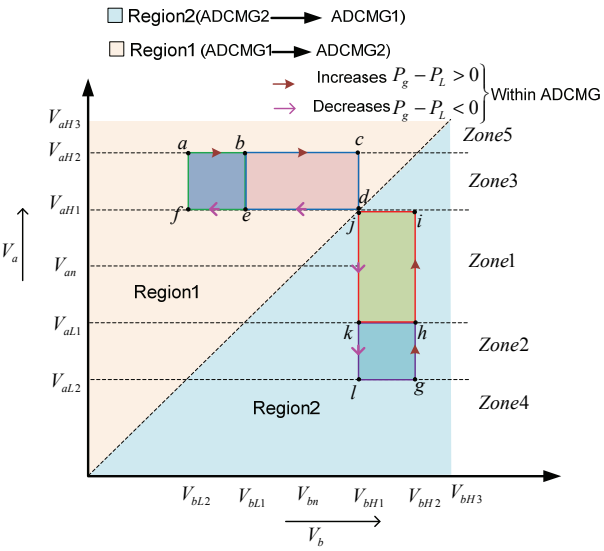

Fig. 3. Proposed PCMS between two ADCMGs.

Where SoC_i, SoC_0, C_N and i_{bat} denotes instantaneous *SoC*, initial *SoC, nominal* capacity and input current of battery respectively. δ is loss coefficient which typically varies in the range of 0.98-1[33].

SoC of battery can be regulated by limiting the charging and discharging currents. Voltage levels envisioned throughout the analysis are in compliance with the paper[34]. Operation of each ADCMG is bifurcated into five zones in which each zone will be active depending upon particular bus voltage threshold as shown in Fig. 3. V_a and V_b are grid voltages of ADCMG1 and ADCMG2. In order to leverage maximum power from PV source, it is operated at maximum power point (MPP) using perturb & observe method in all zones excluding zone-5. PCMS is explained with respect to ADCMG1. Region1 and region2 indicates power flow directions from ADCMG1 to ADCMG2 and ADCMG2 to ADCMG1 respectively. Bisection line used to differentiate the regions of power transfer from one ADCMG to other ADCMG with distinct background colors. Total power generation and load in each ADCMG is indicated by p_g and p_L respectively in Fig.3.

1) Zone-1 (Balanced power mode): As power generated by PV source (p_{PV1}) is more or less equal to demand (p_{L1}) in the ADCMG1 which keeps battery in idle state. Small variations of load and source will not trigger the storage unit in this mode because predefined voltage limits are able to sustain these fluctuations. As there is no fixed source to regulate the bus voltage in this zone, which in turn allow its voltage to vary between the limits V_{aH1} and V_{aL1} that are treated as boundaries of this mode for ADCMG1. Similarly V_{bH1} and V_{bL1} are boundaries for ADCMG2. Neither of the ADCMGs share power to other ADCMG in this zone. Status of various units in ADCMG1 are given by

$$p_{PV1} \cong p_{L1};\ \ p_{bat1} = 0;\ V_{aL1} < V_a < V_{aH1} \qquad (2)$$

Where p_{bat1} is instantaneous battery power in ADCMG1.

2) Zone-2 (Battery discharging mode): As the PV power is

This article has been accepted for publication in a future issue of this journal, but has not been fully edited. Content may change prior to final publication. Citation information: DOI 10.1109/TII.2017.2773507, IEEE Transactions on Industrial Informatics

not sufficient in fulfilling the demand that yields to continuous deviation in bus voltage (V_a). Once V_a fall below threshold value (V_{aL1}) then storage steps into discharging mode from idle state in order to cover the gap between supply and demand. Battery clamps the bus voltage at same threshold (V_{aL1}) by keeping it in bus regulating mode. ADCMG1 is ready to absorb the excess power from ADCMG2 if available (i.e. operating point *h* shown in Fig. 3, but reverse power transfer is not possible. Extreme conditions of battery are taken care in control loop. Equation indicating the conditions of ADCMG1 is given by

$$p_{PV1} + p_{bat1} = p_{L1}; \quad V_a = V_{aL1} \tag{3}$$

3) Zone-3 (Battery charging mode): If the PV source is producing excess power than required, then this mode comes into picture where voltage V_a rises continuously due to surplus power and halts at threshold limit (V_{aH1}) by shifting the battery into charging mode. Battery is allowed to charge until its cutoff limit is met. ADCMG1 cannot feed the power to ADCMG2, but absorb the power from it when V_b is at V_{bH2} and battery1 in ADCMG1 is not fully charged or maximum charging rate is not met (shown as operating point *i* in Fig. 3).

$$p_{PV1} > p_{L1}; \quad p_{bat1} = -(p_{PV1} - p_{L1}); \quad V_a = V_{aH1} \tag{4}$$

4) Zone-4 (Power deficit mode): It is an extension of zone-2 and comes into active state when load rises beyond discharging rate of battery. In this mode, battery runs at maximum discharging current limit. There are two sub cases exist in this zone, in which first case deals with power import from ADCMG2 whereas in the second case, there is no power import from ADCMG2.

Case1: In this case, status of ADCMG2 is checked against surplus power mode by observing its bus voltage V_b. Similarly status of ADCMG1 is known by its bus voltage (V_a). If V_b=V_{bH2} & $V_a \leq V_{aH1}$, then DABC will be triggered to transmit the power from ADCMG2 to ADCMG1 and regulates the voltage of ADCMG2 at V_{bH2}. Transmitted power can push the ADCMG1 to operate at different operating points in dissimilar zones depending on power imported (p_{imp1}) in region2 as shown in Fig. 3 which is explained with following equations

$$V_a = \begin{cases} V_{aL1} & : if \ p_{PV1} + p_{bat1} + p_{imp1} = p_{L1} \\ V_{aL1} < V_a < V_{aH1} & : if \ p_{PV1} + p_{imp1} \cong p_{L1} \\ V_{aH1} & : if \ p_{PV1} + p_{imp1} > p_{L1}, p_{bat1} = -(p_{PV1} + p_{imp1} - p_{L1}) \end{cases} \tag{5}$$

If the first condition in equation (5) is met by ADCMG1 then it will be operated at point *h* in zone-2 shown in Fig. 3. Similarly, once second and third condition is met, then ADCMG1 can be operated between *h* and *i* in zone-1 and at *i* in zone-3 respectively. In contrast to above points, whenever p_{imp1} starts diminishing then operating point will move from *i* to *g*. At any condition if p_{imp1} becomes zero then operating points shift from *i*, *h* to *j*, *k* respectively.

Case2: This case arises when ADCMG2 is not feeding either enough power or zero power to ADCMG1. Hence, load shedding is done as per the priority order in ADCMG1. Load sheds either based on decrement of SoC_1 below cut off limit or falling of voltage V_a below V_{aL2}. In order to avoid the load shedding, non-renewable source is to be activated during above scenarios. Here the operating points *g* and *l* indicate the load shedding of ADCMG1 corresponding to below equation order

$$\begin{aligned} p_{PV1} + p_{bat1} + p_{imp1} < p_{L1} \\ p_{PV1} + p_{bat1} < p_{L1}; p_{imp1} = 0 \end{aligned} \tag{6}$$

5) Zone-5 (Excess power mode): This zone is further split into two sub cases, where one case deals with exporting surplus power from ADCMG1 and another case is without exporting power.

Case1: Either rise in generation or fall in load beyond the charging rate of battery will enforce the ADCMG into this operating zone. If the surplus power is not utilized within the grid then bus voltage starts rising. Status of other ADCMG is observed from its bus voltage in order to dispatch the excess power available. If the ADCMG2 is in a state other than excess power case (i.e. $V_b \leq V_{bH1}$), then power is transferred from ADCMG1 to ADCMG2 displayed as region1 in Fig. 3. If the power is exported from ADCMG1, then bus voltage of ADCMG1 (V_a) is regulated at V_{aH2}. Therefore generated renewable power is efficiently used. ADCMG2 can be operated at (b, c, d, e), (a, f) similar to case1 and case2 in zone-4 depending upon its imported power (p_{imp2}).

Case2: This is an extension of previous case where ADCMG2 is not able to absorb the excess power readily available in ADCMG1 that increase bus voltage (V_a). On the detection of rise in bus voltage (V_a) above V_{aH2}, PV source will shift its operating mode from MPP to bus voltage regulation mode and clamps its bus voltage at V_{aH3}. Status of ADCMG1in zone5 is given by

$$V_a = \begin{cases} V_{aH2} & : if \ p_{exp1} > 0 \\ V_{aH3} & : if \ p_{exp1} = 0 \ \& \ V_{PV1ref} = V_{aH3} \end{cases} \tag{7}$$

Where p_{exp1} and V_{PV1ref} represents instantaneous power exported from ADCMG1 to ADCMG2 and PV voltage reference respectively.

IV. Control Loops

Converter control plays vital role in executing the proposed PCMS for switching the source converters between different modes based on predefined thresholds for triggering. Until and unless the defined threshold voltage is reached by the DC grid, particular mode will not be active because the outer loop is saturated and does not provide any reference to inner loop. Control of battery1 and PV source1 inside the ADCMG1 is elaborated and the similar control structure utilized in ADCMG2 for battery2 and PV source2. Power flow control of IBDC between two DC grids is explained in detail.

A. PV control loop

PV source always remain at MPP except in zone5 irrespective of change in load and power import/export so that maximum renewable power is extracted and utilized efficiently. PV control loop of ADCMG1 is shown in Fig. 4 and the same is followed for PV source in ADCMG2. PV source can be operated in two modes, one as MPP mode and other as bus voltage regulation mode. First one consist of two loops in which outer loop is mainly for tracking MPP voltage (V_{MPP}) through perturb and observe (P&O) method and provides voltage reference as input to inner loop. Inner loop works at faster speed

This article has been accepted for publication in a future issue of this journal, but has not been fully edited. Content may change prior to final publication. Citation information: DOI 10.1109/TII.2017.2773507, IEEE Transactions on Industrial Informatics

for tracking the given reference through PI controller and produce the duty cycle (δ_{pv1}) as its output. Second mode encloses only one loop and comes into picture when case2 of zone-5 occurs. Bus voltage is regulated at its reference (V_{aH3}) through PI controller by adjusting duty cycle. Both the modes use the PWM comparator to generate the required pulses for switches inside the converter by feeding duty cycle to it. Switching between two modes is done selectively by observing the bus voltage. If the V_a increase above the upper threshold V_{aH2}, then PV enter into the bus regulation mode, otherwise PV keeps running in MPP mode. Though battery1 is fully charged, but PV is not pushed into regulation mode since excess power transfer may takes place from ADCMG1 to ADCMG2 for the effective utilization of renewable energy which increases reliability of system.

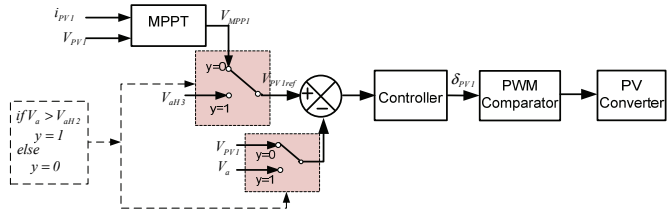

Fig. 4. Control loop of PV source in ADCMG1.

B. Battery control loops

Battery is operated either in charging or discharging modes based on their cut in thresholds. Battery control loop of ADCMG1 is shown in Fig. 5. Each mode employs two loops in which inner loop is common for both the modes. No mode will be active until the bus voltage crosses its predefined threshold value due to saturation of controller. Outer voltage loop mainly tracks bus voltage reference and produces the current reference as output, and that is fed to inner loop for tracking the reference effectively. In discharging mode, top outer loop gives the positive reference current (I_{btrd1}) by regulating bus voltage (V_a) at V_{aL1} as load dominates, which is fed to discharging rate limiter and then checked against its cut off limit (V_{bat1L}) to ensure the optimal utilization and extended battery's life. Cut off limit of $SoC_1 = 20\%$ is expressed in terminal voltage (V_{bat1L})[33]. In this mode, bottom outer loop is inactive. During charging mode, bus voltage is regulated at V_{aH1} through bottom outer loop and produces negative current as reference to inner loop. Here bus voltage always try to rise above the threshold limit (V_{aH1}) in generation dominating scenario. Battery reference current (I_{btrc1}) is checked against charging current limit and full charge (i.e. $SoC_1 = 90\%$) equivalent voltage

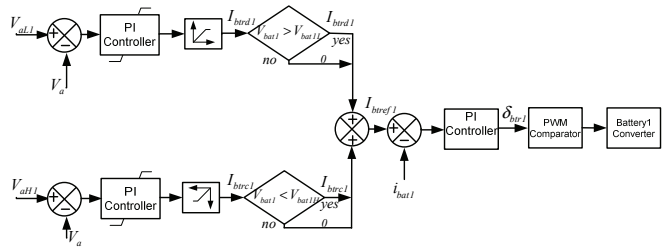

Fig. 5. Control loop of battery in ADCMG1.

V_{bat1H} to avoid high charging rate and over charging condition. Inner control loop track the reference current (I_{btref1}) by changing the duty cycle (δ_{btr1}). In both modes, duty cycle is fed to the PWM comparator for synthesizing the pulses for battery converter.

C. Bidirectional power control between ADCMGs

DABC is employed as bidirectional DC-DC converter (BDC) for transferring the power between ADCMGs. Mainly it works on conventional phase shift method [35]. Power transfer takes place either from ADCMG1 to ADCMG2 or from ADCMG2 to ADCMG1. BDC control is shown in Fig. 6. It consists of two loops in which one is outer voltage loop and other is inner current loop. BDC comes to active state when one of two ADCMGs are possessing the surplus power and other grid is able to absorb. Power transfer from ADCMG2 to ADCMG1 is treated as positive convention and reverse action as negative. If excess energy is available in ADCMG1 and other grid status is examined by its voltage. If other grid is ready (i.e. $V_b \leq V_{bH1}$), then it starts exporting the power by regulating the bus voltage V_a at V_{aH2} through outer voltage controller and provide the negative reference current (I_{bdc2}) which is passed through limiter for avoiding high rush current than absorbing capacity. Then reference current (I_{bdcr}) is tracked by BDC current (i_{bdc}) using inner current controller and generates the required negative phase shift. Similarly while transferring the power from ADCMG2 to ADCMG1, a positive reference current is liberated by regulating the voltage V_b at V_{bH2} through outer loop and is followed by inner loop for synthesizing the positive phase shift. While obtaining the status of ADCMGs by scanning its bus voltage, actual bus voltages are passed through the low pass filter to avoid the false switching.

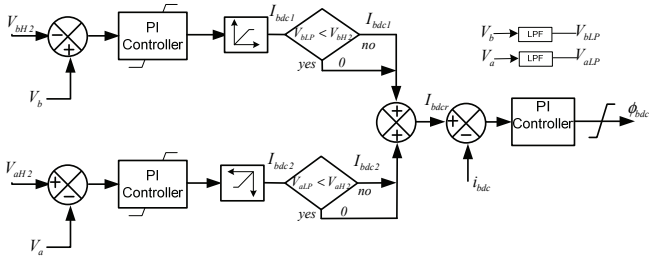

Fig. 6. Control of BDC between two ADCMGs.

D. Load control

Constant power load is developed in this paper by feeding resistive load through the buck converter. Buck converter control is similar to conventional control scheme [36]. Load shedding is performed based on DC bus voltage and battery status as shown in Fig. 7. If the battery voltage falls below cutoff value V_{batL2} (equivalent to $SoC=30\%$) then load shedding is initiated to preserve the battery to feed the essential loads effectively. Similarly if the bus voltage decreases below the lower threshold (V_{aL2}) then load shedding is activated because power deficit exceeds discharging rate of battery. Simultaneously if both occurs during worst scenario, then also it triggers the load shedding. Load can be recovered when bus voltage and battery voltage become higher than their limits (i.e.

This article has been accepted for publication in a future issue of this journal, but has not been fully edited. Content may change prior to final publication. Citation information: DOI 10.1109/TII.2017.2773507, IEEE Transactions on Industrial Informatics

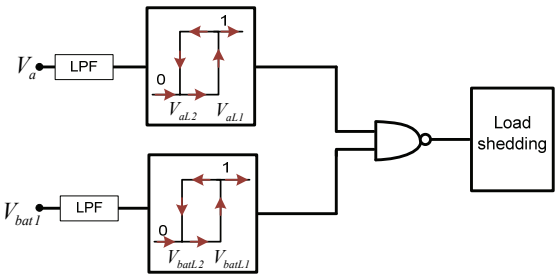

Fig. 7. Load shedding control.

V_{aL1}, V_{batL1} {i.e. *SoC=50%*}). Actual bus voltage and battery terminal voltage are fed through the low pass filter (LPF) to avoid the unwanted switching of load shedding process during sudden increment in load power or decrement in source power.

The proposed PCMS can be extended to multiple similar autonomous DC microgrids operating at same nominal voltages (i.e. V_a and V_b) by utilizing the droop control strategy [12],[13]. It is assumed that same nominal voltage based multiple microgrids can be placed on identical grid voltage side and its cutoff voltages are same as proposed. Power sharing among similar microgrids connected to ADCMG1 and ADCMG2 are given by

$$V_{ai}^{*} = V_{aT} - \alpha_{ai} I_{ai} \tag{8}$$

$$V_{bj}^{*} = V_{bT} - \alpha_{bj} I_{bj} \tag{9}$$

Where V_{aT} is threshold voltage values for all microgrids connected to ADCMG1 side, V_{ai}^{*}, α_{ai} and I_{ai} are output voltage reference set point, droop coefficient and output current of i^{th} ADCMG respectively ($i=1,2,...m$). Similar convention is followed to equation (9) (where $j=1,2,...n$). Droop coefficients α_{ai}, α_{bj} are given by

$$\alpha_{ai} = \frac{V_{aTmax} - V_{aTmin}}{P_{aimax} - P_{aimin}} \tag{10}$$

$$\alpha_{bj} = \frac{V_{bTmax} - V_{bTmin}}{P_{bjmax} - P_{bjmin}} \tag{11}$$

Where V_{aTmax}, V_{aTmin}-Maximum and minimum voltage variation allowed around particular threshold value in common bus of ADCMG1. P_{aimax} and P_{aimin} are maximum power injected and absorbed to/from common bus of ADCMG1 by ith ADCMG of same voltage type respectively. Same convention is followed to equation (11).

This scheme may not be effective and efficient for more than two dissimilar voltages based microgrids since complexity increases with increased number of different voltages based microgrids. Therefore this scheme is economical and reliable for multiple similar ADCMGs (i.e. V_a and V_b voltage based grids) which are very nearer. Complete analysis of multiple ADCMGs will be carried out in future research work.

V. Simulation Results

Simulation of the system shown in Fig. 2 is carried out on real time digital simulator (RTDS) platform to validate the developed PCMS. System is implemented in RSCAD/RTDS environment. Specifications of system components like PV, battery and load in both the ADCMGs are detailed in Table I. Two practical DC grid voltage ratings are chosen to prove the applicability of PCMS. Load is classified as fixed and variable loads based on its existence throughout certain period. They represent the essential and non-essential loads indirectly. Non-essential loads/variable loads are shed according to the requirement and other type is fed continuously. Proposed PCMS is explored under various operating scenarios of ADCMGs including extreme conditions of battery and grid like over charging and discharging, overload and underload scenarios of ADCMG. Operation of individual ADCMGs is illustrated using PCMS under different zones and it is followed by bidirectional power transfer between ADCMGs considering aforementioned conditions in zone-4 and zone-5. As explained in the previous section, bus voltages information of ADCMGs are directly available to BDC for switching between different modes. Typical line length considered here is 1 km and its parameters are listed in Table I.

TABLE I
Simulation Parameters

Components	Parameters	ADCMG1	ADCMG2
PV Capacity	Maximum power @1000W/m^2	4.5 kW	750 W
Battery	Capacity	200 AH	100 AH
	Nominal voltage	96 V	24 V
Nominal grid voltage	Rated voltage	380 V	48 V
Voltage Thresholds	V_{xH3}	410	54 V
	V_{xH2}	400	52 V
	V_{xH1}	390	50 V
	V_{xL1}	370	46 V
	V_{xL2}	360	44 V
DC load	Fixed Load	1 kW	200 W
	Variable Load	2 kW	300 W
Line parameters	Resistance(R)	0.15 Ω	
	Inductance (L)	0.24mH	

* x=a for ADCMG1and x=b for ADCMG2

A. Individual DC microgrids

Various operating regions of ADCMG1 is shown in Fig. 8. Battery terminal voltage is kept just above the lower cut off limit to compile all zones including extreme conditions within the single window. Cutoff limits for each zone are selected with difference of 10V [34] and bus voltage deviation for all zones lie within the ±5% of bus nominal voltage. It is observed from the figure that generated power is equal to load demand from 0 to t_1 that indicates the operating zone-1, during which bus voltage is allowed to vary between boundaries. At time t_1, increase in PV power(p_{PV1}) causes the excess power compared to local demand(p_{L1}) which drive the battery into charging mode from idle state in previous case and starts regulating the bus voltage (V_a) at V_{aH1} which exhibit the zone-3 of ADCMG1. Sudden decrease in variable load appears at t_2 that impel the battery charging current to exceed its saturation limit which causes rise of V_a since surplus power is not consumed by other ADCMG or local load. Thus PV move into bus regulation mode from MPP mode on the detection of rise in V_a above V_{aH2} that is shown as zone-5 in Fig. 8. PV controls the bus voltage V_a at V_{aH3} until t_3 where V_a falls below V_{aH2} due to fall of PV power with decay in irradiation. Again zone-3 appears from t_3 to t_4. At time t_4, rapid increase in load causes the zone-2 to appear

This article has been accepted for publication in a future issue of this journal, but has not been fully edited. Content may change prior to final publication. Citation information: DOI 10.1109/TII.2017.2773507, IEEE Transactions on Industrial Informatics

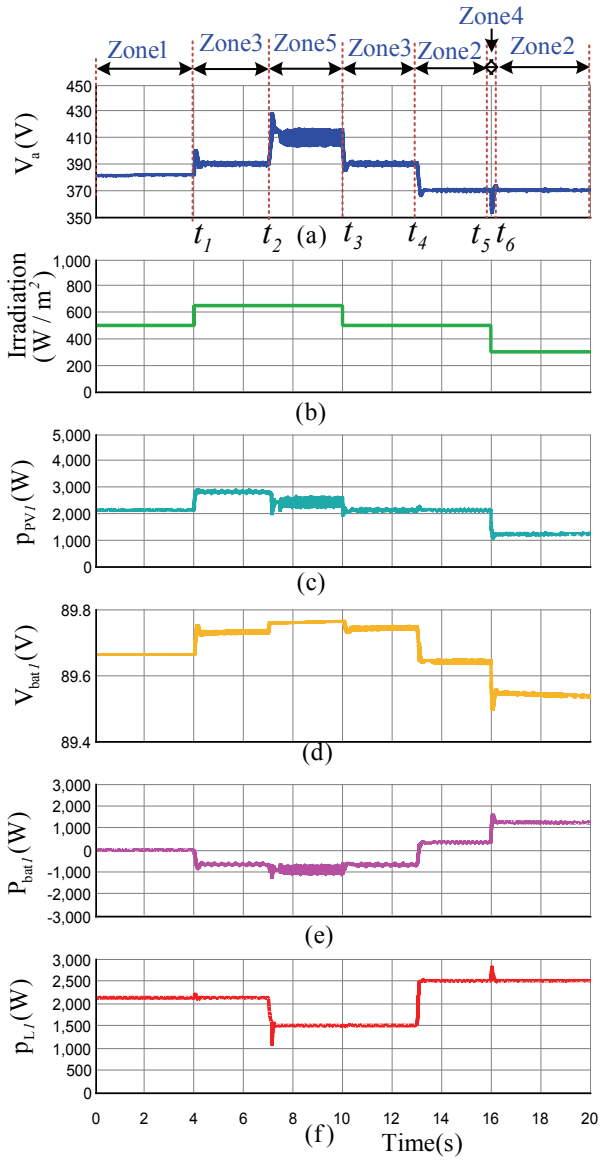

Fig. 8. Operating zones of ADCMG1: (a) Bus voltage, (b) Irradiation, (c) PV output power, (d) Battery terminal voltage, (e) Battery output power, and (f) Load power.

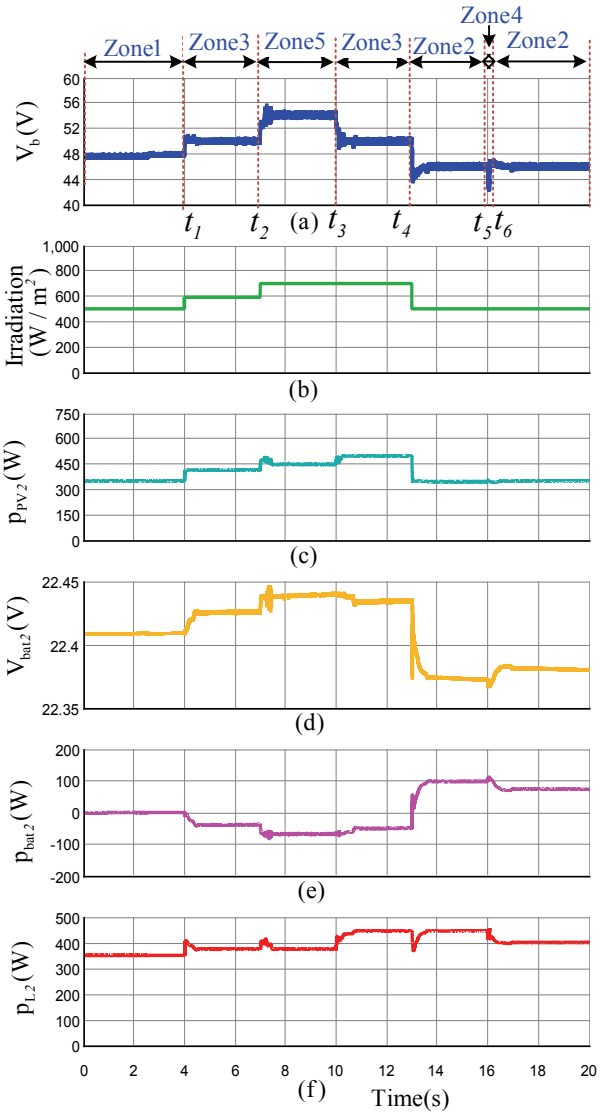

Fig. 9. Operating zones of ADCMG2: (a) Bus voltage, (b) Irradiation, (c) PV output power, (d) Battery terminal voltage, (e) Battery output power, and (f) Load power.

between instants t_4 and t_5 where the demand dominates the generation and battery compensate the difference by shifting from charging to discharging mode instantaneously at t_4 as shown in Fig. 8(e). Further increment in load and fall of irradiation occurs at t_5 that compel battery to discharge more and make bus voltage to fall below its lower cutoff limit (V_{aL2}). Thus load shedding is performed at t_6 to bring back ADCMG1 under normal operating zones. Time interval between t_5 and t_6 reveals the operating zone-4. Once load is shed then it retains the operating zone-2.

Similarly, ADCMG2 is operated with voltage thresholds mentioned in Table I. ADCMG2 follows same sequence of operating zones as that of ADCMG1 as shown in Fig. 9 except Zone-4 in which load sheds when battery terminal voltage falls below its cutoff limit (i.e. $SoC_1 = 30\%$). Though it follows same sequence of zones as ADCMG1 for operation, but power variations inside ADCMG2 is different than ADCMG1 to include wide cases. Aforementioned analysis reveals the effectiveness of the control scheme even under extreme conditions of individual ADCMGs.

B. Inter DC grid power flow

Simulation of inter DC grid power flow using developed PCMS is shown in Fig. 10. From 0 to t_8 , ADCMG1 is operated in zone-3 where the generation dominates the power demand and battery is charging with surplus power as shown in Fig. 10(e). Simultaneously ADCMG2 is in zone-2 with predominant load. Further increase in load occurs at t_7 and clamp the bus voltage V_b at V_{bL1} till t_8 . Sudden rise in PV power (p_{PV1}) inside ADCMG1 at t_8 causes the battery to charge at its saturation current limit due to surplus power which pushes the bus voltage (V_a) to increase further. Once V_a reaches V_{aH2}, then BDC control checks the status of other grid (i.e.ADCMG2). As $V_b \leq V_{bH1}$, then BDC is allowed to deliver the power from ADCMG1 to ADCMG2 by controlling the BDC output current as shown in Fig. 10(c)-(d). Though power is transferred from ADCMG1 to

This article has been accepted for publication in a future issue of this journal, but has not been fully edited. Content may change prior to final publication. Citation information: DOI 10.1109/TII.2017.2773507, IEEE Transactions on Industrial Informatics

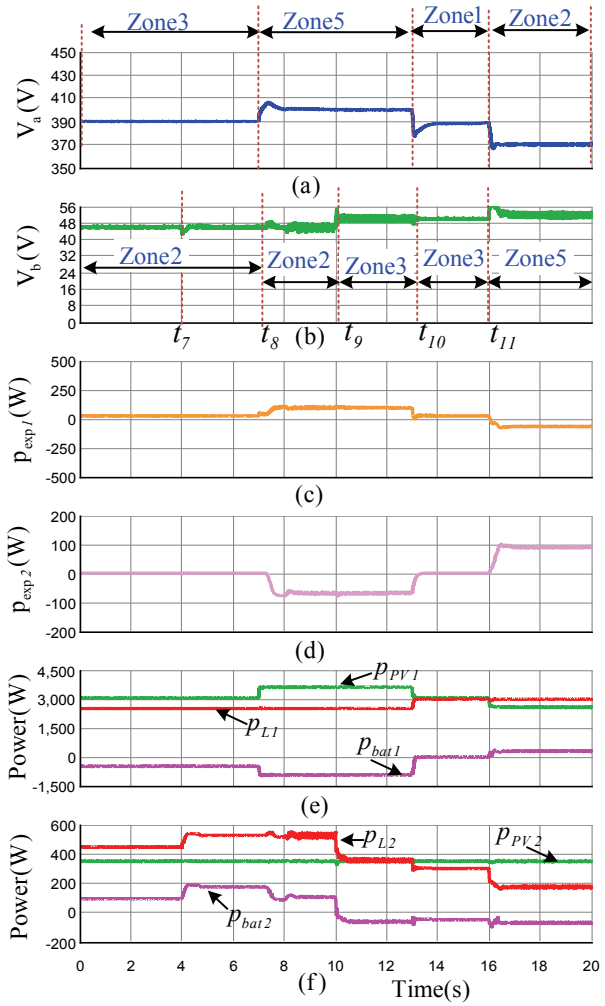

Fig. 10. Operation of BDC using PCMS: (a) ADCMG1 voltage, (b) ADCMG2 voltage, (c) Power exported from ADCMG1, (d) Power exported from ADCMG2, (e) Powers within ADCMG1, and (f) Powers within ADCMG2.

ADCMG2, but ADCMG2 remains to be in zone2 since total available power within ADCMG2 including the power imported from ADCMG1 is less than the demand. Once load falls at time t_9 in ADCMG2, then it jumps into zone-3 from zone-2 as total available power including power imported exceeds the local demand as shown in Fig. 10(b) and (f). At instant t_{10} , sudden fall of p_{PV1} and increment of load inside the ADCMG1 occur simultaneously. This results in ceasing of power export (p_{exp1}) from ADCMG1 as p_{PV1} is sufficient enough to feed the load p_{L1}. Meanwhile load p_{L2} decreases which leads the ADCMG2 to remain in zone-3 till the instant t_{11}. Variations in bus voltage V_a is seen between t_{10} and t_{11} due to minor fluctuations in p_{PV1} while tracking MPP through perturb and observe method. p_{PV1} and p_{L2} decreases simultaneously at time t_{11} that produces surplus power in ADCMG2 beyond its battery charging rate. Therefore BDC control is activated to export the power from ADCMG2 to ADCMG1 (i.e. p_{exp2}) due to rise of V_b above threshold V_{bH2} and at the same time V_a is below V_{aH1} .

In order to validate the effectiveness of PCMS, a comparison is made against configurations from [24], [25] as config-I and config-II respectively in the Table II. It can be observed that proposed configuration finds advantages in terms of increased reliability, flexible control without communication and complexity, effective utilization of resources and storages by enclosing the extreme conditions of battery and ADCMGs.

TABLE II
COMPARISON OF PCMS BASED SYSTEM

Parameter	Config-I [24]	Config-II [25]	Proposed system
Communication	Required	Required	Not required
Control complexity	High	Medium	Low
Isolation	Not Provided	Provided	Provided
Voltage stress of BDC	High	High	Low
Reliability	Low*	Low*	High
Power sharing between DCMGs	Flexible	Not flexible	Flexible

*- with respect to communication based control scheme

VI. EXPERIMENTATION

In order to validate the simulation results, a prototype model is developed. Bus voltage of ADCMG2 remains same as that of simulation, whereas ADCMG1 bus voltage is considered as 100V for experimentation and corresponding voltages thresholds are V_{aH2}=110, V_{aH1}=105, V_{aL1}=95, V_{aL2}=90. Two Programmable DC sources of rating 200V, 40A are configured to mimic the behavior of PV sources. Resistances of range 0-75Ω, 5A are considered for loading the DC grids. Two series connected lead acid batteries with each of rating 12V, 60Ah are used in ADCMG2 and similar rated batteries of four numbers are connected in series within ADCMG1. Bus voltages are sensed by AD202JN isolation amplifier and all source currents are sensed through hall effect Telcon sensors. Proposed scheme is implemented in RTDS to communicate with prototype model via digital and analog input/outputs.

Experimentation is started by operating ADCMG1 and ADCMG2 in zone-3 and zone-2 respectively, where battery1 is charging with excess power available in ADCMG1 and battery2 is discharging to meet the demand in ADCMG2 as shown in Fig. 11. At time t_1, increase in PV1 current produces excess power more than charging rate of battery1 in ADCMG1 that leads to rise in V_a. Mean time ADCMG2 is in battery discharging mode(i.e. zone-2) which can be clearly observable from its bus voltage(i.e. V_b at V_{bL1}) in Fig. 11. Once V_a rises above V_{aH2}, then power export takes place from ADCMG1 to ADCMG2 between t_1 and t_3. ADCMG2 is shifted to zone-1 at t_1 since generation along with imported power equals the demand. As load2 falls at t_2, ADCMG2 is shifted into zone-3 by pushing the battery into charging mode due to surplus power. Increment in load1 at t_3, pushes the ADCMG1 to operate in zone-1 and it stops exporting the power to ADCMG2. At the same time ADCMG2 is shifted into zone-2 since there is no power exchange. Increase in PV2 current at t_4 forces the ADCMG2 to operate in zone-3 where excess power is used to charge battery2. At t_5, decay in PV1 current causes power deficit in ADCMG which is compensated by discharging the battery1 (i.e. zone-2). As PV2 current increases at t_6, this results in surplus power which exceeds the charging rate of battery2 in

This article has been accepted for publication in a future issue of this journal, but has not been fully edited. Content may change prior to final publication. Citation information: DOI 10.1109/TII.2017.2773507, IEEE Transactions on Industrial Informatics

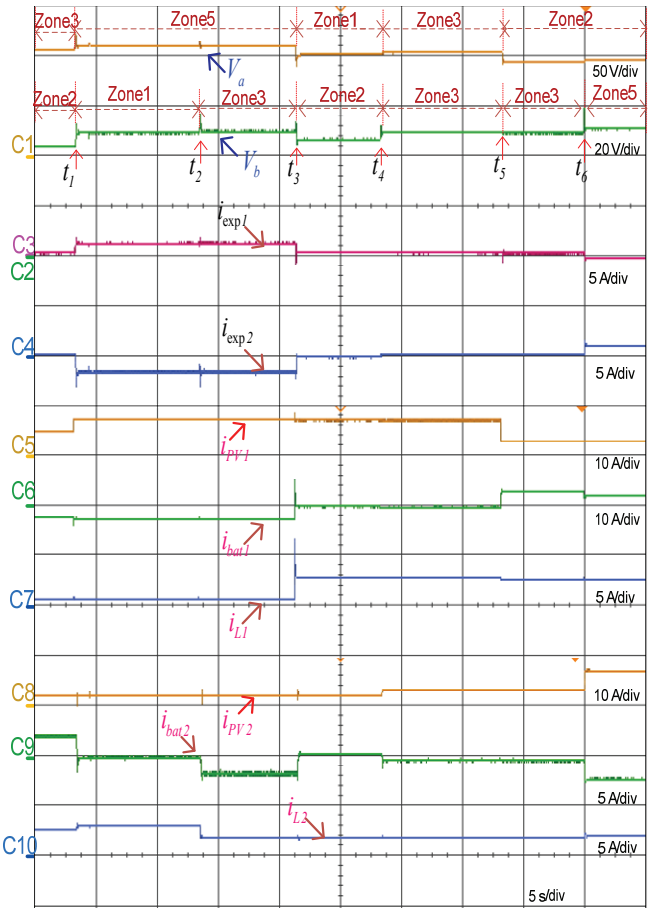

Fig. 11. Experimental results of inter DC grid power flow: Bus voltages (V_a, V_b); current from ADCMG1 to ADCMG2 (i_{exp1}); current from ADCMG2 to ADCMG1 (i_{exp2}); PV source currents (i_{PV1}, i_{PV2}); Battery source currents (i_{bat1}, i_{bat2}); Load currents (i_{L1}, i_{L2}).

ADCMG2, that compel it to export the excess power to ADCMG1.

VII. Conclusion

A PCMS is developed based on bus signaling technique for inter DC grid power flow in case of ADCMGs to increase the system reliability and efficient utilization of resources. Two practical DC grid voltages (380V, 48V) are considered for evaluating the performance of developed scheme in simulation. PCMS is explored under normal and extreme scenarios including the over and under loading conditions of ADCMGs, further more with over charging and discharging of battery. It can be observed from above analysis that proposed PCMS is stable, efficient and effective in realizing communication independent control even under dynamic power variations during the power exchange. This statement is also justified with experimental results obtained through prototype model developed in the laboratory with reduced voltage of ADCMG1. Proposed system provides isolation and also enhances system reliability. Application potential of system suits low and medium voltage customers like domestic consumers, data centers, telecommunication systems, etc. in isolated locations where utility connection is not present or feasible.

Acknowledgement

The authors do acknowledge the financial support provided by Department of Science and Technology (DST), Government of India towards India-UK "HEAPD" research project no: DST/RCUK/SEGES/2012/09(G).

References

[1] T. Dragicevi, X. Lu, J. C. Vasquez, and J. M.Guerrero, "DC Microgrids – Part II: A Review of Power Architectures, Applications and Standardization Issues," *IEEE Trans. Power Electron.*, vol. 31, no. 5, pp. 3528–3549, May. 2016.

[2] Q. Yang, L. Jiang, H. Zhao, and H. Zeng, "Autonomous Voltage Regulation and Current Sharing in Islanded Multi-inverter DC Microgrid," *IEEE Trans. Smart Grid*, vol. PP, no. 99, pp. 1–1, 2017.

[3] J. Torreglosa, P. Garcia, L. Fernandez, and F. Jurado, "Predictive Control for the Energy Management of a Fuel Cell-Battery-Supercapacitor Tramway," *IEEE Trans. Ind. Informat.*, vol. 10, no. 1, pp. 276-285, Feb. 2013.

[4] L. Herrera, W. Zhang, and J. Wang, "Stability Analysis and Controller Design of DC Microgrids with Constant Power Loads," *IEEE Trans. Smart Grid*, vol. 8, no. 2, pp. 881–888, March. 2017.

[5] D. E. Olivares, A. Mehrizi-sani, A. H. Etemadi, C. A. Cañizares, R. Iravani, M. Kazerani, A. H. Hajimiragha, O. Gomis-bellmunt, M. Saeedifard, R. Palma-behnke, G. A. Jiménez-estévez, and N. D. Hatziargyriou, "Trends in Microgrid Control," *IEEE Trans. Smart Grid*, vol. 5, no. 4, pp. 1905–1919, July. 2014.

[6] G. Karina, V. Vagelis, S. Alan, and B. Gabriel, "Optimizing energy savings from' Direct-DC' in US residential buildings," Lawrence Berkeley National Laboratory, Berkeley, CA, Tech. Rep., Oct. 2011.

[7] Schneider Electric, "Indogreen, Telecom Towers Case Study" Tech. Rep. 2014.

[8] EmergeAlliance, "380 Vdc Architectures for the Modern Data Center," Tech. Rep. 2013.

[9] G. S. Seo, J. W. Shin, B. H. Cho, and K. C. Lee, "Digitally controlled current sensorless photovoltaic micro-converter for DC distribution," *IEEE Trans. Ind. Informat.*, vol. 10, no. 1, pp. 117–126, Feb. 2014.

[10] T. L. Vandoorn, B. Meersman, L. Degroote, B. Renders and L. Vandevelde "A Control Strategy for Islanded Microgrids With DC-Link Voltage Control," *IEEE Trans. Power Del.* vol. 26, no. 2, pp. 703–713, April. 2011.

[11] X. Liu, P. Wang, and P. C. Loh, "A Hybrid AC / DC Microgrid and Its Coordination Control," *IEEE Trans. Smart Grid*, vol. 2, no. 2, pp. 278–286, Jun. 2011.

[12] J. John, F. Mwasilu, J. Lee, and J. Jung, "AC-microgrids versus DC-microgrids with distributed energy resources : A review," *Renew. Sustain. Energy Rev. J.*, vol. 24, pp. 387–405, 2013.

[13] J. Schönberger, R. Duke, and S. D. Round, "DC-bus signaling: A distributed control strategy for a hybrid renewable nanogrid," *IEEE Trans. Ind. Electron.*, vol. 53, no. 5, pp. 1453–1460, Oct. 2006.

[14] D. Wu, F. Tang, T. Dragicevic, J. M. Guerrero, and J. C. Vasquez, "Coordinated Control Based on Bus-Signaling and Virtual Inertia for DC Islanded Microgrids," *IEEE Trans. Smart Grid*, vol. 6, no. 6, pp. 1–12, Nov. 2015.

[15] C. Jin, P. Wang, J. Xiao, Y. Tang, and F. H. Choo, "Implementation of hierarchical control in DC microgrids," *IEEE Trans. Ind. Electron.*, vol. 61, no. 8, pp. 4032–4042, Aug. 2014.

[16] J. Xiao, P. Wang, and L. Setyawan, "Multilevel Energy Management System for Hybridization of Energy Storages in DC Microgrids," *IEEE Trans. Smart Grid*, vol. 7, no. 2, pp. 847–856, Mar. 2016.

[17] L. Xu and D. Chen, "Control and Operation of a DC Microgrid With Variable Generation and Energy Storage," *IEEE Trans. Power Deliv.*, vol. 26, no. 4, pp. 2513–2522, Oct. 2011.

[18] D. Chen, L. Xu and L. Yao, "DC voltage variation based autonomous control of DC microgrids," *IEEE Trans. Power Deliv.*, vol. 28, no. 2, pp. 637–648, April. 2013.

[19] T. Dragicevi, J. M.Guerrero, and J. C. C. Vasquez, "A Distributed Control Strategy for Coordination of an Autonomous LVDC Microgrid Based onPower-Line Signaling," *IEEE Trans. Ind. Electron.*, vol. 61, no. 7, pp. 3313–3326, July. 2014.

[20] T. Dragicevic, J. M. Guerrero, J. C. Vasquez, and D. Skrlec, "Supervisory control of an adaptive-droop regulated DC microgrid with battery management capability," *IEEE Trans. Power Electron.*, vol. 29, no. 2, pp.

695–706, Feb. 2014.
[21] S. Adhikari, Q. Xu, Y. Tang, and P. Wang, "Decentralized Control of DC Microgrid Clusters," in *Proc. IFEEC 2017-ECCE Conf. Asia*, 2017, pp. 567–572.
[22] J. Ma, M. Zhu, X. Cai, and Y. W. Li, "Configuration and operation of DC microgrid cluster linked through DC-DC converter," in *Proc. ICIEA Conf.* 2016, pp. 2565–2570.
[23] A. Werth, M. Tokoro, and K. Tanaka, "Bottom-up and recursive interconnection for multi-layer DC microgrids," in *Proc.of Int. Conf. on Environment and Elect. Eng.*, 2016, pp. 1–6.
[24] M. Kumar, S. C. Srivastava, S. N. Singh, and M. Ramamoorty, "Development of a control strategy for interconnection of islanded direct current microgrids," *IET Renew. Power Gener.*, vol. 9, no. 3, pp. 284–296, 2015.
[25] S. Konar and A. Ghosh, "Interconnection of Islanded DC microgrids," in *Proc. IEEE PES APPEEC,* 2015 pp. 1–5.
[26] D. Jovcic and L. Zhang, "LCL DC/DC converter for DC grids," *IEEE Trans. Power Deliv.*, vol. 28, no. 4, pp. 2071–2079, Oct. 2013.
[27] B. Zhao, Q. Yu, and W. Sun, "Extended-phase-shift control of isolated bidirectional DC-DC converter for power distribution in microgrid," *IEEE Trans. Power Electron.*, vol. 27, no. 11, pp. 4667–4680, Nov. 2012.
[28] W. Chen, P. Rong, and Z. Lu, "Snubberless bidirectional DC-DC converter with new CLLC resonant tank featuring minimized switching loss," *IEEE Trans. Ind. Electron.*, vol. 57, no. 9, pp. 3075–3086, Sept. 2010.
[29] M. Lee, W. Choi, H. Kim, and B. H. Cho, "Operation schemes of interconnected DC microgrids through an isolated bi-directional DC-DC converter," in *Proc. IEEE Appl. Power Electron. Conf. and Expo.* 2015, pp. 2940–2945.
[30] S. Moayedi and A. Davoudi, "Distributed Tertiary Control of DC MicrogridClusters," *IEEE Trans. Power Electron.*, vol. 31, no. 2, pp. 1717–1733, Feb. 2015.
[31] M. Yazdanian and A. Mehrizi-Sani, "Distributed control techniques in microgrids," *IEEE Trans. Smart Grid*, vol. 5, no. 6, pp. 2901–2909, Nov. 2014.
[32] S. Piller, M. Perrin, and A. Jossen, "Methods for state-of-charge determination and their applications," *J. Power Sources*, vol. 96, no. 1, pp. 113–120, 2001.
[33] M. Coleman, C. K. Lee, C. Zhu, and W. G. Hurley, "State-of-charge determination from EMF voltage estimation: Using impedance, terminal voltage, and current for lead-acid and lithium-ion batteries," *IEEE Trans. Ind. Electron.*, vol. 54, no. 5, pp. 2550–2557, Oct. 2007.
[34] K. Sun, L. Zhang, Y. Xing, and J. M. Guerrero, "A Distributed Control Strategy Based on DC Bus Signaling for Modular Photovoltaic Generation Systems With Battery Energy Storage," *IEEE Trans. Power Electron.*, vol. 26, no. 10, pp. 3032–3045, Oct. 2011.
[35] C. Mi, H. Bai, C. Wang, and S. Gargies, "Operation, design and control of dual H-bridge-based isolated bidirectional DC–DC converter," *IET Power Electron.*, vol. 6, no. 7, pp. 2846–2852, 2011.
[36] N. Mohan and T. Undeland, "*Power electronics: converters, applications, and design*." John Wiley & Sons, Ltd, 2007.

P Sanjeev (S'16) has completed B.Tech and M.Tech from the CVRCE Hyderabad and National Institute of Technology Bhopal, India, in 2011 and 2013 respectively. He worked as Assistant Professor in Mukesh Patel School of Technology Management and Engineering, NMIMS University Mumbai from 2013 to 2014. Currently he is working as a research scholar under DST sponsored HEAPD Project towards the Ph.D degree at Indian Institute of Technology Roorkee (IITR), India. He received the best paper award at IEEE National conference ICAER held in Punjab University, October 2013. His area of interest includes DC microgrids, Hybrid energy storage systems, and Renewable energy source integration.

Narayana Prasad Padhy (SM'09) received the Ph.D. degree in power systems engineering from Anna University, Chennai, India, in 1997. He is working as a Professor and NEEPCO Chair Professor in the Department of Electrical Engineering, Indian Institute of Technology (IIT) Roorkee, Roorkee, India. He is the National lead of the HEAPD project under India-UK Smart Energy Grid and Energy Storage research initiatives. His research interests are power system analysis, optimization, demand side management and smart grid. He has received the Boyscast Fellowship and the Humboldt Experienced research Fellowship during 2005 and 2009, respectively. He is also a Fellow of the Indian National Academy of Engineers (INAE) and the Institution of Engineering and Technology (IET).

Pramod Agarwal (M'99) received the B.E., M.E., and Ph.D. degrees in electrical engineering from the Indian Institute of Technology Roorkee, Roorkee, India, in 1983, 1985, and 1995, respectively. In 1985, he joined the Indian Institute of Technology Roorkee as a Lecturer, where he is currently a Professor with the Department of lectrical Engineering. During 1999–2000, he was a Postdoctoral Fellow with the Ecole de Technologie Supérieure, University of Quebec, Montreal, QC, Canada. His research interest includes power electronics and smart grid.